

SINGLE PASS COLLIDER MEMO

CN- 251

AUTHOR: John Seeman

DATE: 10/28/83

REPLACES CN#

TITLE: NEW MAGIC ANGLE BUMPS AND MAGIC TRANSLATION BUMPS

SLAC-CN--251

DE84 003222

I. Abstract

SLC beams of opposite charge can be transversely deflected in the same direction by RF fields in the accelerating cavities: sed by girder tilts, coupler-asymmetries, or manufacturing errors. A sy. tric deflection can be corrected by a magic angle bump¹ if the deflection is located adjacent to one of the linac quadrupoles. However, if the deflection is located between quadrupoles, two magic angle bumps or a magic angle bump and a magic translation bump are needed for the correction. Several examples of translation bumps are included. A new magic angle bump is also presented which is longitudinally compressed a factor of two over the one described in Ref. 1 and has significantly reduced particle excursions. Finally, if new correctors are added midway along the girders so that the number of correctors are doubled, then the longitudinal extent and the maximum particle excursion of these new magic bumps can be further reduced.

II. Representation of Symmetric Beam Deflections

A girder in the linac consists of four 10 foot accelerating waveguides each with two couplers. There is a quadrupole on each end. If a girder supports symmetric RF deflecting fields, it is unlikely that the sources of the deflections are adjacent to the quadrupoles. A scheme to represent a kick located arbitrarily along the girder (for example see Fig. 1a) is to rearrange the motion of the beam so that the final results are identical but the actions performed on the beam occur at the quadrupoles where they are computationally easier to handle. For example, the symmetric kick in Fig. 1a can be represented as a kick and a translation at the down stream quadrupole as in Fig. 1b, as a kick and translation at the upstream quadrupole as in Fig. 1c, or as kicks at both the downstream and upstream quadrupoles as in Fig. 1d. Although magic angle bumps are sufficient to correct for an arbitrary symmetric deflection, magic translation bumps may also be useful tools.

NOTICE

PORTIONS OF THIS REPORT ARE ILLEGIBLE.

It has been reproduced from the best available copy to permit the broadest possible availability.

MS
DISTRIBUTION OF THIS DOCUMENT IS UNLIMITED

MASTER

III. Magic Translation Bump

A translation bump must translate an electron beam and a positron beam traveling with the same trajectory parallel to but offset from the axis of the linac back onto that axis. An example of a translation bump is shown in Fig. 2. The displacements of the beam and the incremental deflections along the bump are also tabulated. The key to this bump (as well as the other magic bumps) is that a focusing quadrupole for one beam is a defocusing quadrupole for the oppositely charged beam.

IV. New Magic Angle Bump

A new magic angle bump is shown in Fig. 3. The symmetric kicks given to the beams occur at quadrupole Q_{i+1} located in the center of the bump. The corrector at Q_i separates the beams coming from the left so that they pass through quadrupole Q_{i+1} on opposite sides of the axis. Q_{i+1} deflects both beams equal amounts in the same direction. If the amplitude and sign of the corrector at Q_i are properly chosen, the beam deflections due to Q_{i+1} exactly cancel the deflections caused by the RF. Finally, the correctors at Q_{i+1} and Q_{i+2} direct the beams back to the axis. This bump is a factor of two shorter longitudinally than the one of Ref. 1 and has peak particle amplitudes which are either two or 5.8 times smaller depending on the beam. Furthermore, both beams are handled equally. This bump will significantly reduce the wake field effects on the beams due to the correction of given RF deflections. The maximum corrector strengths are, however, the same for this bump and the one of Ref. 1.

V. "Mid-quad" Correction Scheme

The longitudinal extent of the magic bumps and the transverse maximum particle amplitude of the magic translation bump can be reduced by adding to the linac a second set of correctors placed midway between the present quadrupoles.

VI. Mid-quad Magic Angle Bump

A magic angle bump using the mid-quad correction scheme is shown in Fig. 4. This magic angle bump is very similar to the one of Fig. 3 with the exception that the initial and final correctors are closer to the quadrupoles where the RF kick is located. Clearly, the length of the bump is one half the other bump, but the peak particle excursion is the same. The correctors are twice as strong.

VII. "Mid-quad" Magic Translation Bump

In order to utilize the mid-quad correctors for the magic translation bump, the decomposition of the arbitrary kick in Fig. 1 must be changed. In Fig. 5 is shown a configuration where the translation is performed midway between quadrupoles at the location of a new corrector and the kick is located at the downstream quadrupole. The magic bump which corrects for such a translation is shown in Fig. 6. The translation Δx is included in the middle of the bump. This example is two-thirds the length of the one shown in Fig. 2 and the peak particle amplitude is 0.70: ... large.

Acknowledgements

Discussions with J. Rees, M. Ross, J. Sheppard, and R. Stiening have been very helpful.

Reference

1. R. Stiening, "The Magic Beam Bump", SLAC CN-12, Jan., 1980.

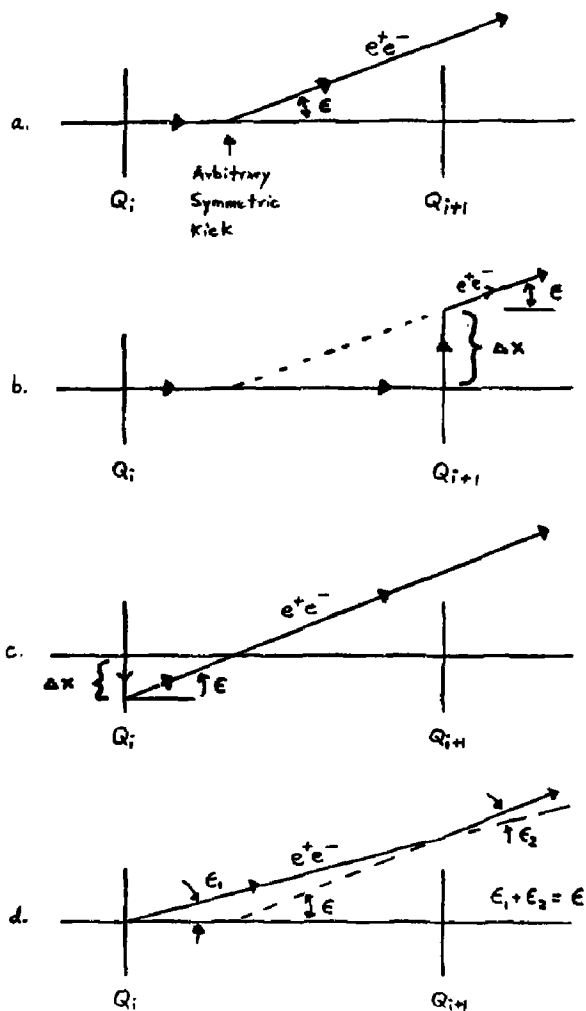
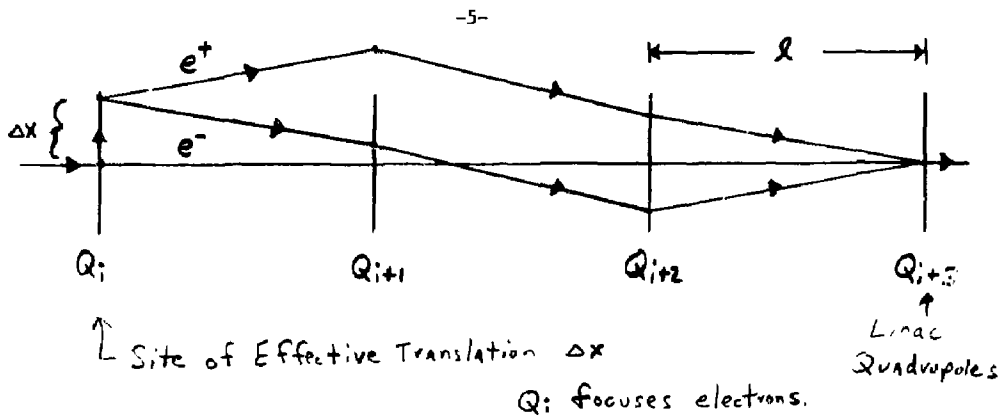


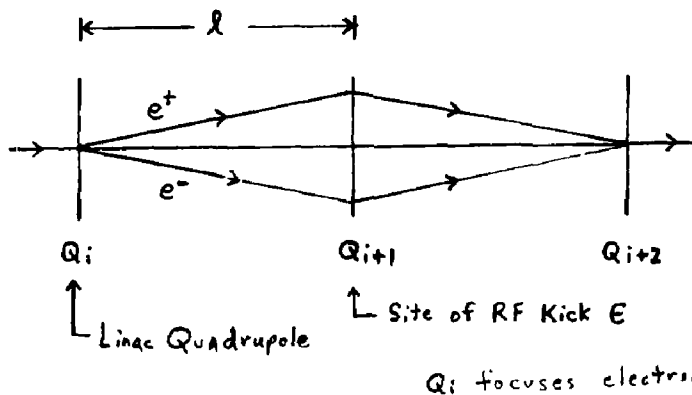
Fig. 1 A symmetric kick may be located between quadrupoles in the SLC linac (see a). This kick may be represented by a kick and a translation at the downstream quadrupole (see b), a kick and a translation at the upstream quadrupole (see c), or kicks at both quadrupoles (see d).

The quadrupole Q_{i+1} is shown to have zero strength only for illustration of the other effects.



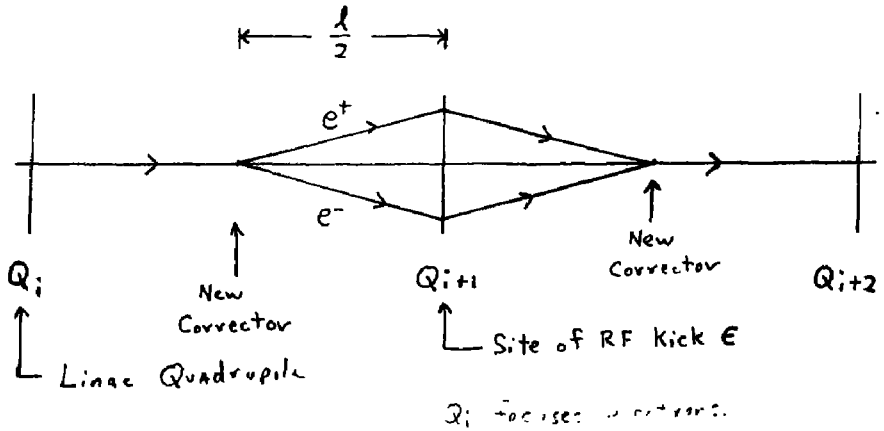
Beam Location	Positrons		Electrons	
	Displacement	Incremental Deflection	Displacement	Incremental Deflection
Q_i	0	0	0	0
Translation Δx at Q_i	$+\Delta x$	0	$+\Delta x$	0
Corr. at Q_i	$+\Delta x$	$\frac{\Delta x}{\sqrt{2}l}$	$+\Delta x$	$-\frac{\Delta x}{\sqrt{2}l}$
Q_{i+1}	$\Delta x \left[1 + \frac{1}{\sqrt{2}} \right]$	$-\frac{\Delta x}{l} [\sqrt{2} + 1]$	$\Delta x \left[1 - \frac{1}{\sqrt{2}} \right]$	$\frac{\Delta x}{l} [\sqrt{2} - 1]$
Corr. at Q_{i+1}	$\Delta x \left[1 + \frac{1}{\sqrt{2}} \right]$	$\frac{\Delta x}{\sqrt{2}l}$	$\Delta x \left[1 - \frac{1}{\sqrt{2}} \right]$	$-\frac{\Delta x}{\sqrt{2}l}$
Q_{i+2}	$\frac{\Delta x}{\sqrt{2}}$	$\frac{\Delta x}{l}$	$-\frac{\Delta x}{\sqrt{2}}$	$\frac{\Delta x}{l}$
Corr. at Q_{i+2}	$\frac{\Delta x}{\sqrt{2}}$	$-\frac{\Delta x}{\sqrt{2}l}$	$-\frac{\Delta x}{\sqrt{2}}$	$\frac{\Delta x}{\sqrt{2}l}$
Q_{i+3}	0	0	0	0
Corr. at Q_{i+3}	0	$\frac{\Delta x}{\sqrt{2}l}$	0	$-\frac{\Delta x}{\sqrt{2}l}$
Q_{i+4}	0	0	0	0

Fig. 2 Magic Translation Bump for 90° per cell FODO lattice. Step translation Δx to both beams at Q_i is compensated in one and one half cells.



Beam Location	Positrons		Electrons	
	Displacement	Incremental Deflection	Displacement	Incremental Deflection
Q_i	0	0	0	0
Corr. at Q_i	0	$\epsilon/\sqrt{2}$	0	$-\epsilon/\sqrt{2}$
Q_{i+1}	$\frac{\epsilon l}{\sqrt{2}}$	$-\epsilon$	$-\frac{\epsilon l}{\sqrt{2}}$	$-\epsilon$
RF Kick at Q_{i+1}	$\frac{\epsilon l}{\sqrt{2}}$	ϵ	$-\frac{\epsilon l}{\sqrt{2}}$	ϵ
Corr. at Q_{i+1}	$\frac{\epsilon l}{\sqrt{2}}$	$-\sqrt{2} \epsilon$	$-\frac{\epsilon l}{\sqrt{2}}$	$\sqrt{2} \epsilon$
Q_{i+2}	0	0	0	0
Corr. at Q_{i+2}	0	$\frac{\epsilon}{\sqrt{2}}$	0	$-\frac{\epsilon}{\sqrt{2}}$

Fig. 3 New Magic Angle Bump for 90° per Cell FODO lattice. The symmetric RF kick ϵ at Q_{i+1} is exactly cancelled by the deflections the beams receive in Q_{i+1} resulting from being on opposite sides of the center line.



Beam Location	Positrons		Electrons	
	Displacement	Incremental Deflection	Displacement	Incremental Deflection
Q_i	0	0	0	0
Corrector between Q_i and Q_{i+1}	0	$\sqrt{2} E$	0	$-\sqrt{2} E$
Q_{i+1}	$\frac{E l}{\sqrt{2}}$	$-E$	$-\frac{E l}{\sqrt{2}}$	$-E$
RF kick at Q_{i+1}	$\frac{E l}{\sqrt{2}}$	E	$-\frac{E l}{\sqrt{2}}$	E
Corr. at Q_{i+1}	$\frac{E l}{\sqrt{2}}$	$-2\sqrt{2} E$	$-\frac{E l}{\sqrt{2}}$	$+2\sqrt{2} E$
Corrector between Q_{i+1} and Q_{i+2}	0	$\sqrt{2} E$	0	$-\sqrt{2} E$
Q_{i+2}	0	0	0	0

Fig. 4 Mid-quad Magic Angle Bump for 90° per cell FODO lattice. The symmetric RF kick is at Q_{i+1} . Additional correctors midway between quadrupoles allows the bump of Fig. 3 to be shortened by a factor of two.

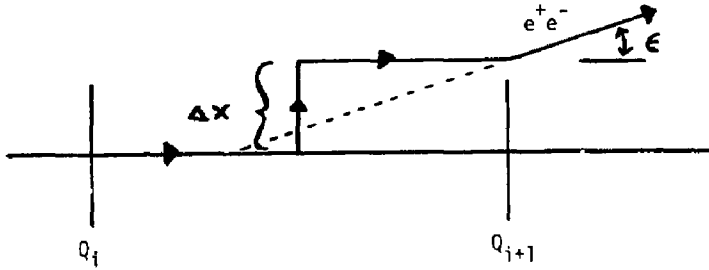
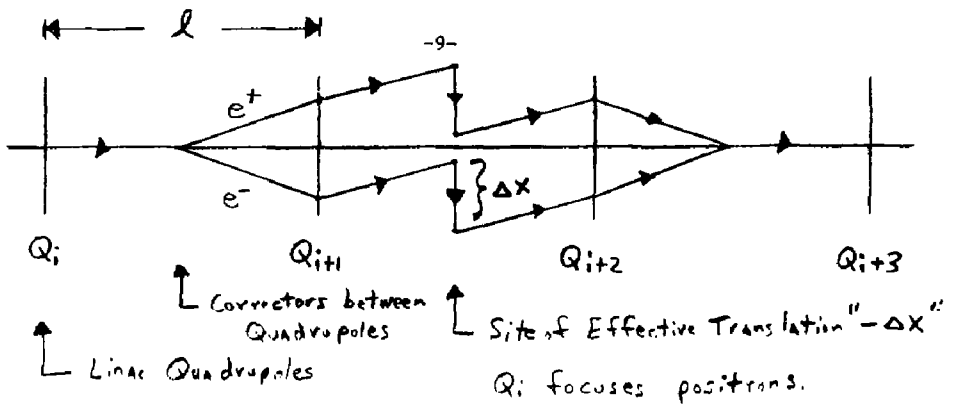


Fig. 5 The symmetric kick shown in Fig. 1a may also be represented as a translation midway between quadrupoles and a kick at the downstream quadrupole. The arrows show the effective motion of the beams. The quadrupole Q_{i+1} is shown to have zero strength only for illustration of the other effects.



Beam Location	Positrons		Electrons	
	Displacement	Incremental Deflection	Displacement	Incremental Deflection
Q_i	0	0	0	0
Corrector between Q_i and Q_{i+1}	0	$\frac{\sqrt{2} \Delta X}{l}$	0	$-\frac{\sqrt{2} \Delta X}{l}$
Q_{i+1}	$\frac{\Delta X}{\sqrt{2}}$	$\frac{\Delta X}{l}$	$-\frac{\Delta X}{\sqrt{2}}$	$\frac{\Delta X}{l}$
Corr. at Q_{i+1}	$\frac{\Delta X}{\sqrt{2}}$	$-\frac{\sqrt{2} \Delta X}{l}$	$-\frac{\Delta X}{\sqrt{2}}$	$\frac{\sqrt{2} \Delta X}{l}$
Corrector between Q_{i+1} and Q_{i+2}	$\Delta X \left[\frac{1}{2} + \frac{1}{\sqrt{2}} \right]$	0	$\Delta X \left[\frac{1}{2} - \frac{1}{\sqrt{2}} \right]$	0
After translation between Q_{i+1} and Q_{i+2}	$\Delta X \left[\frac{1}{\sqrt{2}} - \frac{1}{2} \right]$	0	$-\Delta X \left[\frac{1}{2} + \frac{1}{\sqrt{2}} \right]$	0
Q_{i+2}	$\frac{\Delta X}{\sqrt{2}}$	$-\frac{\Delta X}{l}$	$-\frac{\Delta X}{\sqrt{2}}$	$-\frac{\Delta X}{l}$
Corr. at Q_{i+2}	$\frac{\Delta X}{\sqrt{2}}$	$-\frac{\sqrt{2} \Delta X}{l}$	$-\frac{\Delta X}{\sqrt{2}}$	$\frac{\sqrt{2} \Delta X}{l}$
Corrector between Q_{i+2} and Q_{i+3}	0	$\frac{\sqrt{2} \Delta X}{l}$	0	$-\frac{\sqrt{2} \Delta X}{l}$
Q_{i+3}	0	0	0	0

Fig. 6 Mid-quad Magic Translation Bump for 90° per Cell FODO lattice. By adding midquad correctors and locating the effective beam translation between quadrupoles, the translation bump of Fig. 2 is shortened and reduced in amplitude.

DISCLAIMER

This report was prepared as an account of work sponsored by an agency of the United States Government. Neither the United States Government nor any agency thereof, nor any of their employees, makes any warranty, express or implied, or assumes any legal liability or responsibility for the accuracy, completeness, or usefulness of any information, apparatus, product, or process disclosed, or represents that its use would not infringe privately owned rights. Reference herein to any specific commercial product, process, or service by trade name, trademark, manufacturer, or otherwise does not necessarily constitute or imply its endorsement, recommendation, or favoring by the United States Government or any agency thereof. The views and opinions of authors expressed herein do not necessarily state or reflect those of the United States Government or any agency thereof.